

# Nonrandom Double Strand Cleavage of DNA by a Monofunctional Metal Complex: Mechanistic Studies

Charles A. Detmer III, Filomena V. Pamatong, and Jeffrey R. Bocarsly\*

Department of Chemistry, The University of Connecticut, Storrs, Connecticut 06269

Received May 9, 1996<sup>⊗</sup>

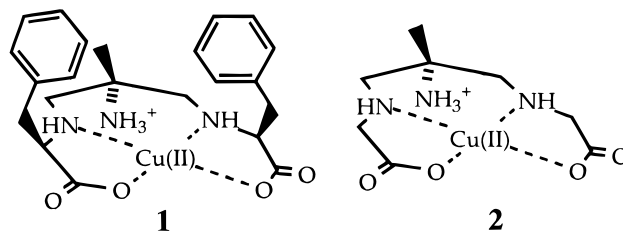
It has been demonstrated in our laboratory that the transition metal complex ((2*S*,8*R*)-5-amino-2,8-dibenzyl-5-methyl-3,7-diazanonanedioato)copper(II) (**1**) is capable of mediating nonrandom double strand cleavage of plasmid DNA. Double strand DNA cleavage is thought to be a biologically significant source of cell lethality and is apparently an important mode of action for both the bleomycin and enediyne classes of antineoplastic agents. We present here the synthesis and characterization of **1** along with mechanistic studies of its DNA scission chemistry. Complex **1**, upon reduction to the Cu(I) state in the presence of O<sub>2</sub>, generates O<sub>2</sub><sup>-</sup> (HO<sub>2</sub>) and O<sub>2</sub><sup>2-</sup> (H<sub>2</sub>O<sub>2</sub>) which react to produce hydroxy radical through the Haber–Weiss reaction. Hydroxy radical is known to abstract hydrogen from deoxyribose, leading to strand scission, release of base propenals, and formation of abasic sites. The pseudo first order kinetics of single strand breakage (*t*<sub>1/2</sub> = 34 min), double strand breakage (*t*<sub>1/2</sub> = 21 min), and base propenal formation (*t*<sub>1/2</sub> = 100 min) have been measured. Base propenal release is therefore kinetically distinct from strand scission, ruling out mechanisms which invoke concerted base propenal formation with strand scission.

## Introduction

Double strand breaks (dsb's) in duplex DNA are thought to be more significant sources of cell lethality than are single strand breaks (ssb's), because they appear to be less readily repaired by DNA repair mechanisms.<sup>1,2</sup> This insight makes the design of molecules that effect double strand cleavage an important goal from the perspective of drug design as well as that of the study of DNA repair mechanisms. We have recently described the design and double strand cleavage chemistry of a copper-based transition metal complex which performs nonrandom double strand cleavage.<sup>3</sup> This process appears to occur by recognition of an abasic-nicked site on duplex DNA by this complex.

Bleomycin is a paradigm for metal complex-mediated non-random double strand cleavage.<sup>4</sup> As illustrated by bleomycin, a transition metal-based double strand cleavage agent must effect four events: nick formation on intact DNA, binding at the nicked site, reactivation, and complementary strand scission to form linear DNA. The design of a molecule which can perform these activities must therefore include a reactivatable metal center and recognition elements that bind both to duplex DNA and at abasic nick sites. For our initial complex (Scheme 1), ((2*S*,8*R*)-5-amino-2,8-dibenzyl-5-methyl-3,7-diazanonanedioato)copper(II) (**1**), we have used phenylalanine to supply the hydrophobic recognition elements. The ligand framework fixes a positively charged ammonium group below the coordination plane of the molecule, with the hydrophobic amino acid side chains constrained to the opposite side of the coordination plane. As a control for the effects of the hydrophobic side chains, we

Scheme 1



have used the glycine-containing version of this molecule, (5-amino-5-methyl-3,7-diazanonanedioato)copper(II) (**2**) (Scheme 1). The rationale behind this molecular architecture is that the ammonium group can interact with phosphates on the DNA backbone, orienting the amino acid side chains toward the bottom of the groove, for interaction with the intact DNA groove or the hydrophobic interior where accessible. Copper(II) has been used extensively in metal-mediated DNA cleavage for the generation of hydrogen-abstrating activated oxygen species<sup>5</sup> and is also capable of DNA cleavage *via* phosphodiester hydrolysis.<sup>6–8</sup> In this report, we describe mechanistic studies of the DNA scission chemistry of complex **1** along with the synthesis of this complex.

## Experimental Section

UV–vis spectra were recorded on an SLM-Aminco Milton-Roy 3000 diode array spectrophotometer. Infrared spectra were recorded as KBr pellets using a Midac M1200 FTIR spectrophotometer. Fluorescence spectroscopy was performed on a Perkin-Elmer λ 3 fluorescence spectrophotometer. pH determinations were performed using a Fisher Scientific pH meter. All materials were reagent grade and were used without further purification unless otherwise noted. Calf thymus (CT)

\* To whom correspondence should be addressed.

⊗ Abstract published in *Advance ACS Abstracts*, October 1, 1996.

- (1) Povirk, L. F. In *Molecular Aspects of Anti-cancer Drug Action*; Neidle, S., Waring, M., Eds.; Verlag-Chemie: Weinheim, Germany, 1983; p 157.
- (2) Povirk, L. F. *Mutat. Res.* **1991**, *257*, 127.
- (3) Pamatong, F. V.; Detmer, C. A., III; Bocarsly, J. R. *J. Am. Chem. Soc.* **1996**, *118*, 5339.
- (4) Natrajan, A.; Hecht, S. M. In *Molecular Aspects of Anticancer Drug-DNA Interactions*; Neidle, S., Waring, M., Eds.; CRC Press: Boca Raton, FL, 1994; Vol. 2, p 197.

- (5) Barton, J. K. In *Bioinorganic Chemistry*; Bertini, I., Gray, H. B., Lippard, S. J., Valentine, J. S., Eds.; University Science Press: Mill Valley, CA, 1994; p 455.

- (6) Kazakov, S. A. In *Bioorganic Chemistry: Nucleic Acids*; Hecht, S. M., Ed.; Oxford University Press: New York, 1996; p 244.
- (7) Linkletter, B.; Chin, J. *Angew. Chem., Int. Ed. Engl.* **1995**, *34*, 472.
- (8) Bashkin, J. K.; Frolova, E. I.; Sampath, U. *J. Am. Chem. Soc.* **1994**, *116*, 5981.

DNA and bovine erythrocyte superoxide dismutase (SOD) were purchased from Sigma. CT DNA was purified using standard procedures.

**Synthesis of 1.**<sup>9</sup> ((2*S*,8*R*)-2,8-Dibenzyl-5-methyl-5-nitro-3,7-diazononanedioato)copper(II)<sup>10</sup> (9.84 g, 20 mmol) was slurred with Zn powder (13.08 g, 200 mmol) in dimethylformamide (DMF) (40 mL); 20% concentrated HCl (v/v, 40 mL) was added, and the reaction was heated on a water bath (~95 °C) with stirring for 1 h. The reaction was then cooled and filtered, and the pH was raised to 11.6 with a saturated NaOH solution. The resulting zinc hydroxide was filtered from solution. The pH was adjusted to 9 with concentrated HCl. Cu(NO<sub>3</sub>)<sub>2</sub>·2.5H<sub>2</sub>O (9.32g, 40 mmol) was added, and the pH was adjusted again to 3 with concentrated HCl. Microcrystalline solid precipitated at room temperature and was filtered from solution, washed with dilute HCl, and allowed to air dry. A 2.81 g amount was collected (yield 28%). Anal. Calcd for 1<sup>+</sup>Cl<sup>-</sup>·DMF·2H<sub>2</sub>O (C<sub>25</sub>H<sub>39</sub>N<sub>4</sub>O<sub>7</sub>CuCl): C, 49.50; H, 6.48; N, 9.24. Found: C, 49.41; H, 6.51; N, 9.16.

**Synthesis of 2.** Compound 2 was synthesized using the literature procedure.<sup>9-11</sup>

**(a) Electrophoresis.** Agarose gel electrophoresis was performed using 1% agarose gels under standard conditions. Samples, usually 20 μL, were run on horizontal gels using 100 mM tris, 100 mM borate, and 2 mM Na<sub>2</sub>EDTA (EDTA = ethylenediaminetetraacetic acid) (pH 8) as buffer. Electrophoresis was continued typically for 60 min at 12 V/cm. After electrophoresis, gels were ethidium stained and destained and then visualized under UV light.

**(b) DNA Scission Conditions.** Electrophoresis experiments were performed with pUC18 DNA; all other experiments were done using calf thymus DNA. Scission reactions were performed at room temperature as follows: pUC18 DNA, 12.5 μM DNA base pairs (bp), 100 μM metal complex, 190 μM ascorbate/peroxide in 20 mM phosphate buffer, pH 7.0; calf thymus DNA, 260 μM DNA base pairs; 640 μM metal complex; 1.3 mM ascorbate/peroxide in 20 mM phosphate buffer, pH 7.0. Reaction was quenched by addition of EDTA. Quantitation by electrophoresis (strand scission events) or visible absorbance (base propenal release) was then performed. Base propenal was quantified by reaction with 2-thiobarbituric acid.<sup>12</sup>

Densitometric quantitation was performed using a Macintosh Quadra 950 equipped with NIH Image software.<sup>13</sup> Supercoiled plasmid DNA values were corrected by a factor of 1.3, on the basis of average literature estimates of lowered binding of ethidium to this structure.<sup>14,15</sup>

**(c) Hydroxy Radical Assay by 2-Deoxy-D-ribose Degradation.** Hydroxy radical production by 1 was assayed by degradation of 2-deoxy-D-ribose followed by quantitation of 2-thiobarbituric acid adduct.<sup>12</sup> A 100 μM amount of metal complex was reacted at room temperature with 1.0 mM 2-deoxy-D-ribose with activation by either 190 μM sodium ascorbate or 190 μM H<sub>2</sub>O<sub>2</sub> and sodium ascorbate. Reactions were performed in a 4 mL volume of 20 mM phosphate buffer (pH 7.0). Parallel runs containing hydroxy radical quenchers dimethyl sulfoxide (DMSO), ethanol, or thiourea (1 mM) were run under identical conditions. Runs with superoxide dismutase contained 50 μL of 1 mg/mL SOD (3300 units/mg). Anaerobic trials were run under the same concentration conditions described above in septum-equipped vials or cuvettes after ca. 20 min of N<sub>2</sub> purging. Reaction solutions were quenched with EDTA (2.4 mM final concentration) and

stored on ice. Each aliquot was then reacted with 2-thiobarbituric acid at 95 °C for 15 min. Workup was identical for all trials. The chromophore concentration was measured by fluorescence intensity at 553 nm (532 nm excitation). Fluorescence intensity was used due to its sensitivity and due to the fact that ascorbate byproducts absorb in the visible region, interfering with visible quantitation of the thiobarbituric acid adduct. Fluorescence intensity was converted to concentration with a standard fluorescence curve constructed using known concentrations of the chromophore, synthesized from malondialdehyde and 2-thiobarbituric acid.<sup>16</sup> Blank reactions lacking cleavage agent were included in each run, and the blank intensity was subtracted from each experimental point.

**(d) Hydroxy Radical Assay by Rhodamine B Degradation.**

Hydroxy radical production was quantitated using rhodamine B<sup>17</sup> (6 μM) as reporter molecule in the presence of 100 μM 1 in a thermostated cuvette at 25 °C with activation by either 190 μM sodium ascorbate or 190 μM each H<sub>2</sub>O<sub>2</sub> and sodium ascorbate. Degradation of dye was monitored at 552 nm (ε = 10.7 × 10<sup>4</sup> M<sup>-1</sup> cm<sup>-1</sup>). Reactions were performed in a 2.2 mL volume of 20 mM phosphate buffer (pH 7.0). Parallel runs containing ethanol (2 mM) as hydroxy radical quencher were performed under identical conditions. Anaerobic runs were performed in a stopcock-equipped cuvette after extensive purging of the reaction mixture with N<sub>2</sub> prior to addition of N<sub>2</sub>-purged activating agents. Runs in the presence of OH<sup>•</sup> quencher were used to ascertain that rhodamine B is not reactive with other activated oxygen species (such as O<sub>2</sub><sup>-</sup>), since the observation of full quenching in the presence of OH<sup>•</sup> quenchers implies that no other dye-reactive species are present. Spectra of ~6 μM rhodamine B with 100 μM 1 were identical to those of the dye in the absence of metal complex, suggesting that rhodamine B does not effectively coordinate to the metal center of 1 under the conditions used. Anaerobic reactions using FeCl<sub>3</sub> and H<sub>2</sub>O<sub>2</sub> (Fenton conditions) with rhodamine B were used to verify that the dye degrades in the presence of hydroxy radical and in the absence of dioxygen.

**(e) Quantitation of Reduced 1, [1·Cu<sup>I</sup>], Formed during DNA Scission.** The visible absorbance of 1 (100 μM) was monitored at 622 nm (thermostated cuvette at 25 °C) during the course of reaction with CT DNA (10 μM bp) using sodium ascorbate/H<sub>2</sub>O<sub>2</sub> tandem activation (190 μM each). The absorbance was converted to concentration using the measured extinction coefficient (85.3 M<sup>-1</sup> cm<sup>-1</sup>), and the measured values were subtracted from the initial concentration of 1 to obtain the amount of copper(I) complex formed.

## Results

Complex 1 was synthesized by a variation of the literature method used for similar complexes.<sup>9-11</sup> The visible spectrum for 1 is typical for Jahn–Teller distorted copper(II) complexes, with an estimated extinction coefficient of 85.3 M<sup>-1</sup> cm<sup>-1</sup> at 622 nm in 20 mM phosphate buffer, pH 7.0. The complex follows Beer's law in the concentration range used (up to 1.3 mM), suggesting that no dimerization occurs in aqueous buffer (inset, Figure 1). Copper(II) is generally either five- or six-coordinate with Jahn–Teller distorted axial sites. The parent structure of 1, complex 2, exhibits a square pyramidal geometry with an apical chloride ligand in its crystal structure (Cu–Cl bond length, 2.63 Å).<sup>10</sup> Complex 1 is likely to be structurally analogous; in addition, steric blockage of one face of the molecule by the phenylalanine side chains is possible, which would enforce a square pyramidal coordination geometry. The complex geometry is therefore thought to be square pyramidal, with an aqua ligand in the apical site. Visible spectra of the complex (100 μM) were recorded (pH 7.0, phosphate buffer) in the presence of the ligands thiourea, DMSO, or ethanol (1

(9) Comba, P.; Hambley, T. W.; Lawrance, G. A.; Martin, L. L.; Renold, P.; Varnagy, K. *J. Chem. Soc., Dalton Trans.* **1991**, 277.

(10) Balla, J.; Bernhardt, P. V.; Buglyo, P.; Comba, P.; Hambley, T. W.; Schmidlin, R.; Stebler, S.; Varnagy, K. *J. Chem. Soc., Dalton Trans.* **1993**, 1143.

(11) Comba, P.; Curtis, N. F.; Lawrance, G. A.; Sargeson, A. M.; Skelton, B. W.; White, A. H. *Inorg. Chem.* **1986**, 25, 4260.

(12) Halliwell B.; Gutteridge, J. M. C. In *CRC Handbook of Methods for Oxygen Radical Research*; Greenwald, R. A., Ed.; CRC Press: Boca Raton, FL, 1985, p 177.

(13) The NIH Image program (written by Wayne Rasband at the U. S. National Institutes of Health and available from the Internet by anonymous ftp from zippy.nimh.nih.gov or on floppy disk from NTIS, 5285 Port Royal Rd., Springfield, VA 22161; part number PB93-504868) is public domain software.

(14) Hertzberg, R. P.; Dervan, P. B. *J. Am. Chem. Soc.* **1982**, 104, 313.

(15) Mirabelli, C. K.; Huang, C.-H.; Crooke, S. T. *Cancer Res.* **1980**, 40, 4173.

(16) Burger, R. M.; Berkowitz, A. R.; Peisach, J.; Horwitz, S. B. *J. Biol. Chem.* **1980**, 255, 11832.

(17) Farhatziz, Ross, A. B. *Selected Specific Rates of Reactions of Transients from Water in Aqueous Solution. III Hydroxyl Radical and Perhydroxyl Radical and Their Radical Ions*; NSRDS-NBS 59, U. S. Department of Commerce/National Bureau of Standards: Washington, D.C., 1977; p 59.

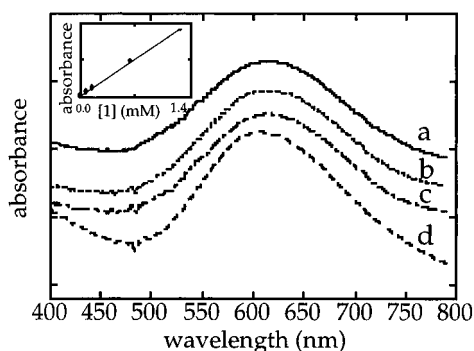


**Figure 1.** Visible spectra of **1** in phosphate buffer (20 mM, pH 7.0) with added ligands: (a) 100  $\mu\text{M}$  **1**; (b) 100  $\mu\text{M}$  **1** + 1 mM DMSO; (c) 100  $\mu\text{M}$  **1** + 1 mM ethanol; (d) 100  $\mu\text{M}$  **1** + 1 mM thiourea. Ordinate offsets are arbitrary. Inset: Beer's law plot of **1**.

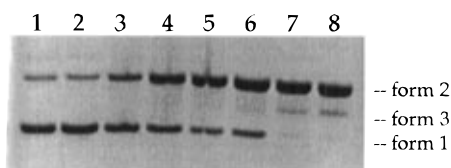


**Figure 2.** Agarose gel electrophoresis of cleavage reaction of pUC18 DNA by **1** (ethidium staining). Scission conditions: 12.5  $\mu\text{M}$  DNA base pairs; 100  $\mu\text{M}$  metal complex; 190  $\mu\text{M}$  ascorbate/peroxide in 20 mM phosphate buffer; pH 7.0. Lane 1: DNA control. Lane 2: DNA + **1** control. Lanes 3–8, reaction after 5, 10, 20, 30, 60, and 90 min of reaction. (Image reversed for clarity.)

mM) in order to determine if any detectable spectroscopic shifts occur to indicate coordination of these exogenous ligands. As shown in Figure 1, the spectra of complex **1** with DMSO (Figure 1b) and ethanol (Figure 1c) are indistinguishable from the complex with no added ligand (Figure 1a), with  $\lambda_{\text{max}}$  for these species at  $\sim 622$  nm. In the presence of thiourea (Figure 1d), an asymmetry appears in the absorbance peak and a marked shift in  $\lambda_{\text{max}}$  to  $\sim 608$  nm occurs. This suggests that apical coordination about the copper(II) square plane by DMSO or ethanol does not occur in aqueous buffer and that this site is occupied by an aqua ligand. Thiourea, as evidenced by Figure 1d, appears to coordinate, presumably at the apical coordination site.

**Kinetic Studies of DNA Scission Chemistry.** The DNA strand scission chemistry of **1** has been kinetically characterized by quantitation of single strand break formation, double strand break formation, base propenal release, and hydroxy radical formation. The formation of ssb's and dsb's was quantitated by gel electrophoresis (Figure 2) on plasmid DNA, and the average numbers of single strand breaks ( $n_1$ ) and double strand breaks ( $n_2$ ) per molecule were quantitated using the standard model, which assumes a Poisson distribution of cleavage sites.<sup>18–20</sup> The release of base propenal during strand scission was quantitated using 2-thiobarbituric acid as the reporter molecule. Figure 3 shows the mass fractions of DNA species present during reaction under relatively mild reaction conditions. Figure 4 is a first order kinetic plot of single and double strand break formation during cleavage by **1**. As shown, the kinetics

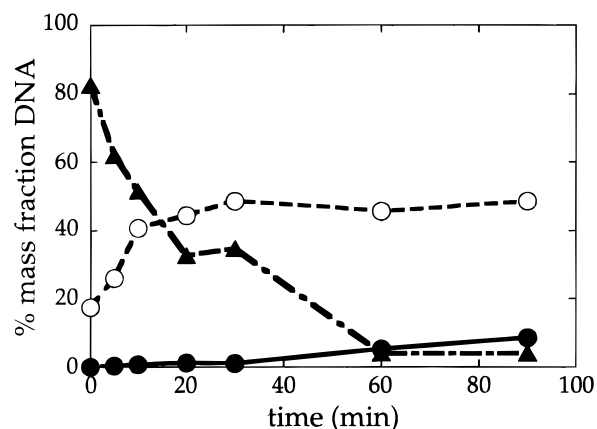


**Figure 3.** Mass fractions of DNA species during cleavage reaction of pUC18 plasmid with **1**:  $\blacktriangle$ , form I supercoiled DNA;  $\circ$ , form II nicked DNA;  $\bullet$ , form III linear DNA.

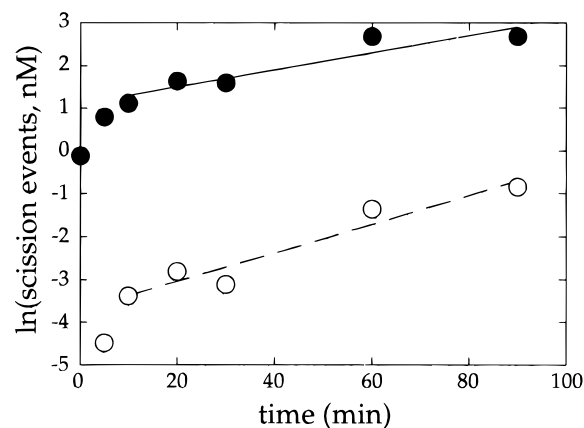


**Figure 4.** First order kinetic plot of formation of single strand breaks and double strand breaks during cleavage of pUC18 plasmid DNA:  $\bullet$ , single strand breaks;  $\circ$ , double strand breaks. Solid lines: linear least squares fits of data beyond induction period.

**Table 1.** Pseudo First Order Kinetic Parameters for ssb, dsb, and Base Propenal Formation

species	$k$ ( $\text{min}^{-1}$ )	$t_{1/2}$ (min)	DNA
ssb	0.0201	34.5	pUC18
dsb	0.0333	20.8	pUC18
base propenal	0.0069	100	CT

of both ssb and dsb formation approximate first order behavior after an induction period of approximately 15 min. Linear least squares fits of the data beyond the induction period give half-lives of 34 min for ssb formation and 21 min for dsb formation (Table 1). These  $t_{1/2}$  values for ssb and dsb formation may not be experimentally distinct, given the degree of scatter of the points.

The data for base propenal release during strand scission chemistry is presented in Figure 5. This reaction shows approximate first order kinetics beyond the induction period, similar to ssb and dsb formation in Figure 4. Since base propenals of all four bases are most likely formed, the observed first order behavior is most likely due to the low kinetic resolution of the assay, although accidental near-equality of rates of formation of the different base propenals in this system is possible. It is also possible that the rate of base propenal release reflects a single first order rate limiting step, independent of the specific base propenal formed. The  $t_{1/2}$  value for this reaction (100 min) is significantly longer than that for the strand scission events, as shown in Table 1. Base propenal release is therefore kinetically resolved from strand scission.

(18) The fraction of linear DNA after scission chemistry,  $f_{\text{III}} = n_2 \exp(-n_2)$ . The fraction of supercoiled remaining after treatment is  $f_{\text{I}} = \exp[-(n_1 + n_2)]$ .<sup>19</sup> The Freifelder–Trumbo relation is  $n_2 = n_1^2(2h + 1)/4L$ , where  $h$  is the maximum separation in base pairs between two cuts on complementary strands that produce a linear DNA molecule ( $h = 16$ ), and  $L$  is the number of phosphoester bonds per DNA strand in the plasmid ( $L = 2686$ , [pUC18]).<sup>20</sup>

(19) Povirk, L. F.; Wubker, W.; Kohnlein, W.; Hutchinson, F. *Nucleic Acids Res.* **1977**, *4*, 3573.

(20) Freifelder, D.; Trumbo, B. *Biopolymers*, **1969**, *7*, 681.

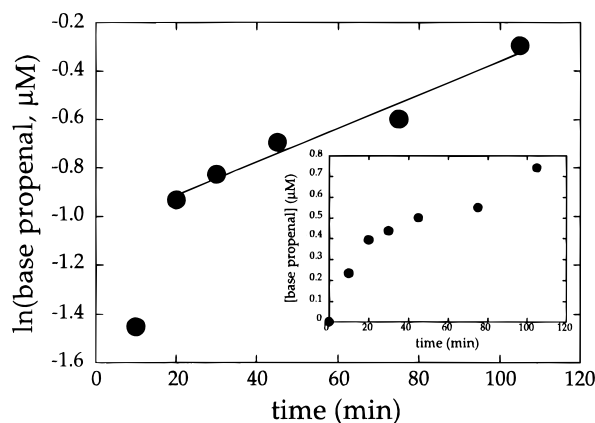


**Figure 5.** First order kinetic plot of base propenal release during cleavage of calf thymus DNA with complex **1**. Solid line: linear least squares fit of data beyond induction period. Inset: release of base propenal as a function of time during cleavage of calf thymus DNA with **1**.

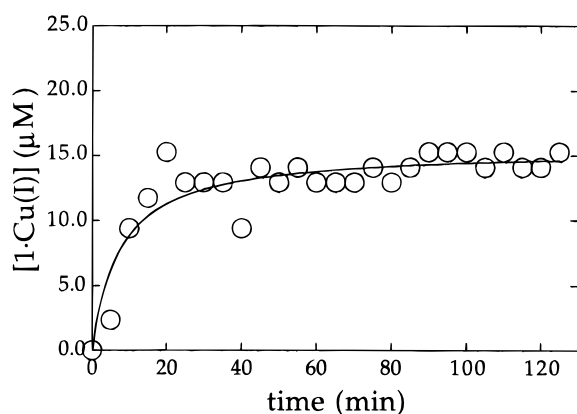


**Figure 6.** Concentration of activated **1**,  $1 \cdot \text{Cu}^{\text{I}}$ , formed during reaction. Reaction conditions: **1** ( $100 \mu\text{M}$ ), sodium ascorbate and  $\text{H}_2\text{O}_2$  ( $190 \mu\text{M}$  each), CT DNA ( $10 \mu\text{M}$  bp) in phosphate buffer (pH 7.0).

**Quantitation of Reduced **1**,  $[1 \cdot \text{Cu}^{\text{I}}]$ , Formed during DNA Scission.** In order to establish an upper limit on the amount of active copper species during the course of reaction, the amount of copper(I) complex formed during reaction was determined by monitoring the visible peak for copper(II). As shown in Figure 6, under the standard reaction conditions used for DNA scission in this study ( $100 \mu\text{M}$  **1**,  $190 \mu\text{M}$  ascorbate/ $\text{H}_2\text{O}_2$ ,  $10 \mu\text{M}$  DNA bp), a steady state of ca.  $15 \mu\text{M}$  copper(I) complex is reached after an induction period of about 15 min.

**Active Oxidant.** In order to obtain information about the active chemical species which effects DNA damage, we have looked for the formation of the activated oxygen intermediates hydroxy radical and superoxide. Hydroxy radical release by complex **1** was assayed using two different radical traps, 2-deoxy-D-ribose<sup>12</sup> or rhodamine B.<sup>17</sup> 2-Deoxy-D-ribose provides a chemically equivalent model for the oxidative target in DNA strand scission chemistry. Rhodamine B provides a target with a high rate constant for reactivity with  $\text{OH}^\bullet$  ( $\sim 10^9 \text{ M}^{-1} \text{ s}^{-1}$ )<sup>17</sup> along with the advantage of direct quantitation of reaction by electronic spectroscopy. Quantitation by 2-deoxy-D-ribose under conditions of sodium ascorbate activation appears in Figure 7. The values found can be compared to the amount of  $\text{OH}^\bullet$  formed during tandem ascorbate/ $\text{H}_2\text{O}_2$  activation (Figure 7).<sup>3</sup> Approximately equal amounts of  $\text{OH}^\bullet$  form ( $\sim 13 \text{ nM}$ ) on activation with sodium ascorbate alone as those that form when both ascorbate and  $\text{H}_2\text{O}_2$  are present. However, quantitation of  $\text{OH}^\bullet$  by rhodamine B (Figure 8) indicates that tandem activation with hydrogen peroxide and ascorbate raises the

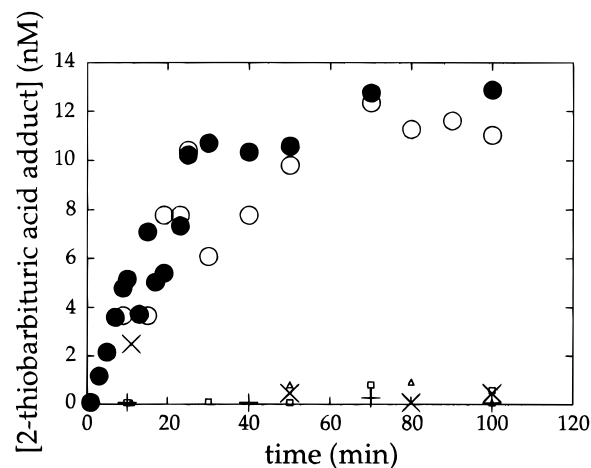


**Figure 7.** Assay of hydroxy radical production by 2-deoxy-D-ribose ( $1 \text{ mM}$ ) by formation of 2-thiobarbiturate with **1** ( $100 \mu\text{M}$ ) in pH 7.0 phosphate buffer. Reaction conditions: ●, activation by sodium ascorbate alone ( $190 \mu\text{M}$ ); ○, activation with both  $\text{H}_2\text{O}_2$  and sodium ascorbate ( $190 \mu\text{M}$  each)<sup>3</sup>; □, quenching of ascorbate/ $\text{H}_2\text{O}_2$  reaction by ethanol ( $1 \text{ mM}$ ); +, quenching of ascorbate activated reaction by ethanol ( $1 \text{ mM}$ ); △, quenching of ascorbate/ $\text{H}_2\text{O}_2$  reaction by DMSO ( $1 \text{ mM}$ ); ×, quenching of ascorbate/ $\text{H}_2\text{O}_2$  reaction by thiourea ( $1 \text{ mM}$ ).

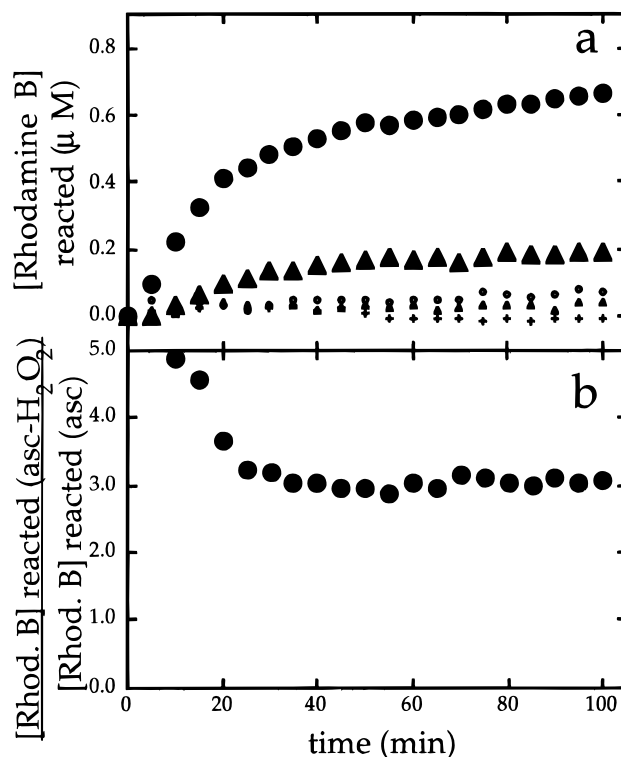


**Figure 8.** (a) Assay of hydroxy radical production by rhodamine B ( $6 \mu\text{M}$ ) with **1** ( $100 \mu\text{M}$ ) in pH 7.0 phosphate buffer. Reaction conditions: ●, aerobic activation with both  $\text{H}_2\text{O}_2$  and sodium ascorbate ( $190 \mu\text{M}$  each); ▲, aerobic activation with sodium ascorbate ( $190 \mu\text{M}$ ); ○, anaerobic activation with both  $\text{H}_2\text{O}_2$  and sodium ascorbate ( $190 \mu\text{M}$  each); △, anaerobic activation with sodium ascorbate ( $190 \mu\text{M}$ ); +, quenching of reaction (ascorbate activation) by ethanol ( $2 \text{ mM}$ ). (b) Ratio of rhodamine B reacted with exogenous  $\text{H}_2\text{O}_2$  (ascorbate +  $\text{H}_2\text{O}_2$  activation) to that in the absence of  $\text{H}_2\text{O}_2$  (ascorbate activation); average of two trials.

production of hydroxy radicals from  $\sim 200 \text{ nM}$  (activation by ascorbate alone) to  $\sim 700 \text{ nM}$  (tandem activation with ascorbate/ $\text{H}_2\text{O}_2$ ). The sizable difference in the amount of radical trapped by these two different methods presumably reflects differences in the trapping reactions, since there may be kinetic differences between the reactions, and because only a subset of the hydrogen

**Table 2.** Quantitation of Hydroxy Radical Formation by **1** with 2-Deoxy-D-ribose Trapping in the Presence and Absence of SOD or O<sub>2</sub><sup>a</sup>

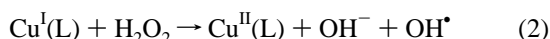
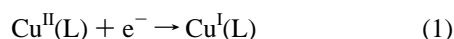
time (min)	[thiobarbituric acid adduct] (nM)					
	ascorbate/H <sub>2</sub> O <sub>2</sub>	ascorbate	ascorbate/H <sub>2</sub> O <sub>2</sub> + SOD	ascorbate + SOD	ascorbate/H <sub>2</sub> O <sub>2</sub> - O <sub>2</sub>	ascorbate - O <sub>2</sub>
5	0.0	1.7	0.0	0.0	0.0	0.24
15	0.64	5.6	0.0	0.0	0.0	0.0
30	5.1	8.5	0.0	0.15	0.0	0.0
45			0.24	0.0		
50	8.1	8.4			0.0	0.0
90	9.2		0.0	0.0		
100	9.0	10.2			0.0	0.0

<sup>a</sup> Reaction conditions: 100 μM **1**, 190 μM activating agents, 1 mM 2-deoxy-D-ribose in 20 mM phosphate buffer (pH 7.0).

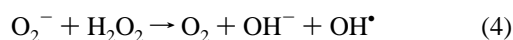
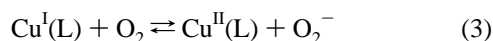
abstractions from deoxyribose produces thiobarbituric-reactive material. In addition, the quantitation of OH• radical by rhodamine must be considered a lower limit on the amount actually formed, since other OH• reaction pathways (e.g., reaction with buffer, self-quenching) have not been quantitated.

Because active oxidants other than hydroxy radical (such as metal-oxo species) can lead to ribose degradation products indistinguishable from those formed by OH•, we examined our reaction in the presence of three known hydroxy radical quenchers, thiourea, DMSO, and ethanol (Figures 7 and 8). In all cases, the reaction is suppressed, regardless of whether both activating agents or ascorbate alone are used. This suggests that the active oxidant is indeed hydroxy radical. However, since the quenchers used are all also ligands, inhibition of reaction may occur not by radical quenching, but by blocking of the coordination site on copper that is involved in radical formation. As noted above, the visible spectra of **1** in the presence and absence of DMSO or ethanol are identical (Figure 1), so suppression of reaction by coordination appears not to occur with these quenchers, but by true OH• quenching. Thiourea, however, effects a change in the visible spectrum of **1**, and may inhibit reaction in part by blocking the coordination site at which the OH• precursor binds.

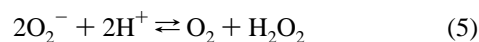
Hydroxy radicals are generated by a variety of chemical and physical processes. Transition metal mediated OH• production is known to occur by a number of routes; two well-known pathways are the Fenton mechanism and the Haber-Weiss mechanism. In the Fenton mechanism, the metal ion acts as a catalyst for hydroxy radical generation from hydrogen peroxide:



The Haber-Weiss reaction (eq 4)<sup>21</sup> involves the reaction of superoxide with H<sub>2</sub>O<sub>2</sub> to produce dioxygen, hydroxide, and OH•:



The production of O<sub>2</sub><sup>-</sup> during reaction does not preclude a Fenton mechanism, however, since dismutation of O<sub>2</sub><sup>-</sup> to dioxygen and H<sub>2</sub>O<sub>2</sub> can occur:



We attempted to quantitate the amount of superoxide formed during the reaction using a standard reductive colorimetric assay for O<sub>2</sub><sup>-</sup> (nitro blue tetrazolium<sup>22,23</sup>). However, in initial studies, we found that, under anaerobic conditions, both sodium

ascorbate or reduced **1** have the ability to reduce the dye molecule directly. Similar problems with competing redox reactions have been noted with colorimetric assays for O<sub>2</sub><sup>-</sup>.<sup>24</sup> We then attempted to detect the formation of superoxide during reaction by adding SOD to the reaction mixture. Only reactions which proceed through an O<sub>2</sub><sup>-</sup> intermediate should be affected by the presence of the enzyme. As can be seen in Table 2, reaction is effectively quenched by the presence of SOD, indicating that O<sub>2</sub><sup>-</sup> is an intermediate in the production of OH•.

The role of dioxygen in radical trapping by deoxyribose was then investigated by conducting the reaction under anaerobic conditions with either ascorbate activation or tandem ascorbate/H<sub>2</sub>O<sub>2</sub> activation. As can be seen from the data in Table 2, the exclusion of molecular oxygen under either set of activation conditions effectively suppresses the formation of trapped product. While these results are consistent with the requirement of O<sub>2</sub> and O<sub>2</sub><sup>-</sup> as participants in OH• formation, they do not constitute confirmation. The suppression of reaction under anaerobic conditions may result not from the failure to abstract a proton from deoxyribose but rather from the lack of O<sub>2</sub> to react with the deoxyribose radical formed *via* proton abstraction, which leads to thiobarbituric-reactive products.<sup>25</sup> Degradation of rhodamine B by OH•, however, does not require O<sub>2</sub> in the degradation pathway. Anaerobic reaction of OH• formation by **1** does not produce any degradation of rhodamine (Figure 8). This confirms the requirement of O<sub>2</sub> as reactant in the generation of hydroxy radical by **1** in the presence or absence of H<sub>2</sub>O<sub>2</sub>.

## Discussion

Under activation conditions of ascorbate alone or ascorbate/H<sub>2</sub>O<sub>2</sub>, the full quenching of reaction by known hydroxy radical quenchers implies that **1** cleaves DNA by generation of OH• and not *via* formation of metal-oxo intermediates. Metal-oxo species have been invoked in copper-mediated oxidative chemistry<sup>26</sup> and are expected to exhibit DNA cleavage chemistry similar to that of OH•, but are not expected to be quenched by hydroxy radical quenchers.<sup>27</sup> However, participation of metal-oxo species has not been ruled out experimentally. In addition, a "Fenton-like" copper(I)-peroxo intermediate has been invoked in copper-mediated proton abstraction and could play a role in reaction.<sup>28</sup>

The full inhibition of reaction by addition of SOD (Table 2) allows both the Fenton and the Fenton-like copper-peroxo

(21) Haber, F.; Weiss, J. *Proc. R. Soc. London, Ser. A* **1934**, *147*, 332.

(22) Nakayama, T.; Kimura, T.; Kodama, M.; Nagata, C. *Carcinogenesis* **1983**, *4*, 765.

(23) Auclair, C.; Voisin, E. In *CRC Handbook of Methods for Oxygen Radical Research*; Greenwald, R. A., Ed.; CRC Press: Boca Raton, FL, 1985; p 123.

(24) Weiss, R.; Flickinger, A. G.; Rivers, W. G.; Hardy, M. M.; Aston, K. W.; Ryan, U. S.; Riley, D. P. *J. Biol. Chem.* **1993**, *268*, 23049.

(25) Stubbe, J.; Kozarich, J. W. *Chem. Rev.* **1987**, *87*, 1107.

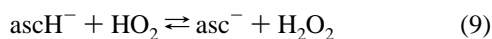
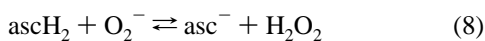
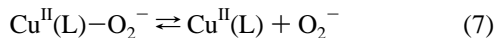
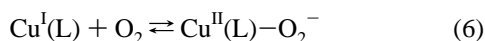
(26) Kitajima, N.; Koda, T.; Iwata, Y.; Moro-oka, Y. *J. Am. Chem. Soc.* **1990**, *112*, 8833.

(27) Rodriguez, L. O.; Hecht, S. M. *Biochem. Biophys. Res. Commun.* **1982**, *104*, 1470.

(28) Masarwa, M.; Cohen, H.; Meyerstein, D.; Hickman, D. L.; Bakac, A.; Espenson, J.H. *J. Am. Chem. Soc.* **1988**, *110*, 4293.

mechanisms to be ruled out and the Haber–Weiss mechanism to be favored for production of  $\text{OH}^\bullet$  by **1**. The effect of added SOD (under either set of activating conditions) is to divert  $\text{O}_2^-$  from the reaction sequence, leaving reducing agent and  $\text{H}_2\text{O}_2$  in the presence of **1**. These are classic Fenton conditions (reduced **1** +  $\text{H}_2\text{O}_2$ ), and essentially no product forms. Therefore, no Fenton or copper–peroxide intermediates appear to form. Furthermore, anaerobic tandem activation of **1** with ascorbate/ $\text{H}_2\text{O}_2$  in the presence of rhodamine B also constitutes Fenton conditions. Rhodamine B does not require  $\text{O}_2$  for formation of degradation products, and no measurable degradation is observed. This is confirmatory evidence that no hydroxy radical is produced under these conditions within the limits of the measurement. Thus, two independent assays both exclude the Fenton (or related copper–peroxo) pathway for hydroxy radical production by **1**. Given the involvement of  $\text{O}_2^-$  as indicated by the SOD studies, we conclude that **1** generates hydroxy radical through the Haber–Weiss pathway. This also excludes the “Fenton–Haber–Weiss” reaction;<sup>29</sup> however, the possibility of metal participation in Haber–Weiss chemistry remains.

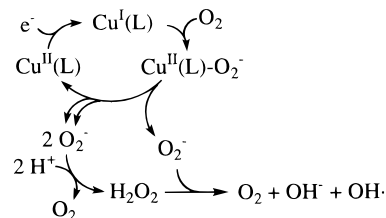
The Haber–Weiss reaction requires sources of both  $\text{O}_2^-$  and  $\text{H}_2\text{O}_2$  to form  $\text{OH}^\bullet$  (eq 4). The simplest sequence of steps which leads to release of  $\text{O}_2^-$  is shown by eqs 6 and 7. Exogenous reductant (either ascorbate or  $\text{H}_2\text{O}_2$ ) produces Cu(I) which generates  $\text{O}_2^-$  from  $\text{O}_2$ . Peroxide forms by dismutation of  $\text{O}_2^-$ , eq 5 (with the possibility of involvement of **1** in dismutation). Alternately,  $\text{O}_2^-$  may react with ascorbate to produce hydrogen peroxide (eqs 8 and 9).<sup>30</sup> Generation of  $\text{H}_2\text{O}_2$  is followed by the Haber–Weiss reaction (eq 4) to release hydroxy radical.



Kinetically, the Haber–Weiss reaction is likely slower than production of  $\text{H}_2\text{O}_2$ ; rate constants measured for the uncatalyzed reaction have been measured most recently at 0.13<sup>31</sup> and 2.25  $\text{M}^{-1} \text{s}^{-1}$ .<sup>32</sup> This can be compared to rate constants measured for the aqueous dismutation of  $\text{O}_2^-$ , which depend on the protonation state of superoxide ( $\text{p}K_{\text{a}} \sim 4.8$ ):  $\text{HO}_2 + \text{O}_2^-$  ( $k = 9.7 \times 10^7 \text{ M}^{-1} \text{ s}^{-1}$ ) and  $\text{O}_2^- + \text{O}_2^-$  ( $k < 0.3 \text{ M}^{-1} \text{ s}^{-1}$ ).<sup>29</sup> Additionally, reaction of ascorbate with  $\text{O}_2^-$  affords  $\text{H}_2\text{O}_2$  by two routes (eqs 8 and 9), with a combined rate constant of  $k = 1 \times 10^7 \text{ M}^{-1} \text{ s}^{-1}$ .<sup>30</sup>

Starting with Cu(II) and dioxygen, three electrons are required to reach the Haber–Weiss products  $\text{OH}^- + \text{OH}^\bullet$ . In the case of activation of **1** by ascorbate alone (i.e., no exogenous  $\text{H}_2\text{O}_2$ ), this means that three equivalents of  $\text{O}_2^-$  must be produced for every equivalent of hydroxy radical, two of which dismute to form  $\text{H}_2\text{O}_2$  while the third reacts with  $\text{H}_2\text{O}_2$  to form  $\text{OH}^\bullet$ . When exogenous  $\text{H}_2\text{O}_2$  is added, all superoxide produced can react to form  $\text{OH}^\bullet$  in a 1:1 stoichiometry. This is reflected in the plateau region of Figure 8, where the ratio of  $\text{OH}^\bullet$  quantified under

## Scheme 2



conditions of ascorbate/ $\text{H}_2\text{O}_2$  activation to that produced under activation with ascorbate alone is  $\sim 3:1$  (Figure 8b). The overall mechanistic proposal is summarized in Scheme 2.

The final concentration (at ca. 90 min of reaction) of hydroxy radical by **1** under the conditions of DNA strand scission (tandem activation by ascorbate/ $\text{H}_2\text{O}_2$ ) is approximately 13 nM (Figure 7) as quantitated by 2-deoxy-D-ribose (1 mM) and  $\sim 700$  nM as quantitated by rhodamine B (6  $\mu\text{M}$ ). The latter measurement places a lower limit on the amount of  $\text{OH}^\bullet$  actually formed. The level of DNA strand scission events (initial DNA concentration, 10  $\mu\text{M}$  DNA bp) at this time point as quantitated by gel electrophoresis with ethidium staining is  $\sim 14.5$  nM single strand breaks and 0.4 nM double strand breaks (Figure 4). In addition, we have previously found that abasic sites opposite to nicks form in a  $\sim 1:1$  ratio to dsb's.<sup>3</sup> This requires a total of  $\sim 15$  nM hydroxy radical to account for the observed DNA lesions formed during scission chemistry. Complex **1** clearly produces ample amounts of hydroxy radical to account for the DNA scission events observed in this system.

Quantitation of the amount of reduced **1** shows that there is a steady-state concentration of  $\sim 15 \mu\text{M}$  reduced **1** during the course of reaction, or about 1000 times the actual number of strand scission events quantitated and about 20 times the amount of  $\text{OH}^\bullet$  trapped with rhodamine B. Thus, the overall production of strand scissions for this system is not limited by the availability of reduced complex. Since the actual amount of reduced and activated **1** bound to DNA during reaction is not known, an estimate of the number of strand scissions per equivalents of active **1** currently cannot be made.

Mechanistic studies of the DNA strand scission chemistry of a classic related system, bis(*o*-phenanthroline)copper(II), have indicated that this system follows a different mechanistic pathway.<sup>33</sup> Reduction of the copper to the cuprous state leads to the generation of  $\text{O}_2^-$ , as observed for **1**. In this system, it is thought that superoxide dismutates to  $\text{H}_2\text{O}_2$ , which then reacts with another equivalent of cuprous ion through a version of the Fenton mechanism to produce hydroxy radical-like species, which may be metal-bound. This species, which may be considered analogous to a metal–oxo system, is responsible for initiating DNA strand scission chemistry.<sup>34</sup> The differences between the two systems are likely related to the electronic differences between the two complexes, including the  $\pi$  characteristics of phenanthroline *vs* the  $\sigma$  character of the ligand of **1**, and to the different geometries available to the two systems.

Based on the data presented here, the general mechanism for scission of the DNA backbone by **1** appears to involve the following steps. First, **1** binds to the intact DNA surface either in activated or unactivated form (followed by activation if necessary) and produces diffusible  $\text{OH}^\bullet$  through generation of  $\text{O}_2^-$  and  $\text{H}_2\text{O}_2$  intermediates. This is followed by hydroxy radical-mediated hydrogen abstraction from deoxyribose. The deoxyribose radicals formed react to form strand scission

(29) Bensasson, R. B.; Land, E. J.; Truscott, T. G. *Excited States and Free Radicals in Biology and Medicine*; Oxford University Press: Oxford, U.K., 1993; p 111.

(30) Cadenas, E. In *Oxidative Stress and Antioxidant Defenses in Biology*; Ahmad, S., Ed.; Chapman & Hall: New York, 1995; p 30.

(31) Weinstein, J.; Bielski, B. H. J. *J. Am. Chem. Soc.* **1979**, *101*, 58.

(32) Ferradini, C.; Foes, J.; Houee, C.; Pucheault, J. *Photochem. Photobiol.* **1978**, *28*, 697.

(33) Graham, D. R.; Marshall, L. E.; Reich, K. A.; Sigman, D. S. *J. Am. Chem. Soc.* **1980**, *102*, 5419.

(34) Sigman, D. S. *Acc. Chem. Res.* **1986**, *19*, 180.

products. Radiolytically generated OH• has been shown to abstract hydrogen from the C4' position of deoxyribose in DNA oligomers.<sup>35</sup>

The evidence presented above shows that base propenal release is a kinetically distinct event from strand scission events, as has been observed for bleomycin cleavage of DNA.<sup>36,37</sup> Therefore, a concerted release of base propenal with strand scission does not occur during DNA cleavage by **1**; rather, a "long-lived" base propenal precursor appears to form as in bleomycin-mediated strand scission.<sup>37</sup> However, the kinetics of strand scission by **1** vs that by bleomycin differ. Bleomycin has a  $t_{1/2}$  of ~2–4 min for ssb formation, a  $t_{1/2}$  ~ 5 min for dsb, and a  $t_{1/2}$  ~ 40 min for base propenal release.<sup>36</sup> Under the conditions of cleavage employed in this study, the strand scission reaction is much slower than the bleomycin-mediated reaction. In addition, the difference in time scale between base propenal release and strand scission is also smaller for **1** than for bleomycin, with the half-life of base propenal release only 3–5 times as long as that for the strand scission events. These time scales differ by about an order of magnitude in bleomycin studies.<sup>36</sup> It is not surprising that strand scission kinetics should differ for **1** compared to bleomycin, since the two systems are mechanistically distinct. However, it is not clear why rates of base propenal release should differ, since strand scission chemistry by **1** is faster than base propenal release in bleomycin-mediated strand scission.

Cleavage at the complementary strand by **1** to effect double strand cleavage presumably occurs by a similar mechanism. Two limiting mechanistic schemes can be envisioned. Complex **1**

either remains bound at the site of the initial nick for reactivation or diffuses out of the initial nick site and nick binding by **1** from bulk solution occurs. Activation of nick-bound complex results in hydroxy radical release and cleavage at the opposing strand. Since our data support a diffusible oxidant, there is no requirement to invoke a second binding mode for **1** for cleavage to occur at the complementary strand. Data previously developed in our laboratory (the observation of a linear relationship between  $n_2$  and concentration of **1** over a range of 50–200  $\mu\text{M}$ )<sup>3</sup> has been taken as support for the first scenario. The kinetic data presented above for ssb and dsb formation are also consistent with the first scenario, in which **1** remains bound at the nick site after nicking, for reactivation and complementary strand cleavage. This is because even if the  $t_{1/2}$  values for dsb and ssb formation are within experimental error of one another, the second scenario requires two completely independent binding, recognition and activation cycles from bulk solution, while the first requires only a single binding event from bulk solution. The second scenario should therefore be a slower process than the first (assuming that binding is the rate-limiting step). The possible equivalence of these two values therefore supports a single binding and recognition event by one complex that achieves either single or double strand cleavage. If the rate of dsb formation is in fact faster than the rate of ssb formation, the same conclusion is supported (however, binding would not be the rate-limiting step). While our evidence thus far favors the first scenario, either mechanistic picture for double strand cleavage requires molecular recognition by **1** of an abasic-nicked site on the DNA surface to mediate cleavage at the complementary strand.

**Acknowledgment.** We would like to acknowledge helpful discussions with Prof. C. V. Kumar.

IC960519P

(35) Kuwabara, M.; Ohshima, H.; Sato, F.; Ono, A.; Matsuda, A. *Biochemistry* **1993**, *32*, 10599.

(36) Burger, R. M.; Projan, S. J.; Horowitz, S. B.; Peisach, J. *J. Biol. Chem.* **1986**, *261*, 15955.

(37) McGall, G. H.; Rabow, L. E.; Ashley, G. W.; Wu, S. H.; Kozarich, J. W.; Subbe, J. *J. Am. Chem. Soc.* **1992**, *114*, 4958.